Title
Fluorescence lifetime detection with particle counting devices.

Journal
Biomedical Optics Express, 10(3)

ISSN
2156-7085

Authors
Hedde, Per Niklas
Abram, Tim
Vu, Tam
et al.

Publication Date
2019-03-01

DOI
10.1364/boe.10.001223

Peer reviewed

Research Article | Vol. 10, No. 3 | 1 Mar 2019 | BIOMEDICAL OPTICS EXPRESS 1223
Biomedical Optics EXPRESS

Fluorescence lifetime detection with particle counting devices

Per Niklas Hedde,[1] Tim Abram,[2] Tam Vu,[3] Weian Zhao,[3] and Enrico Gratton[1,*]

[1]*Laboratory for Fluorescence Dynamics, Department of Biomedical Engineering, University of California Irvine, Irvine, CA, USA*
[2]*Velox Biosystems, 5 Mason St, Ste 160, Irvine, CA 92618, USA*
[3]*Sue and Bill Gross Stem Cell Research Center, Chao Family Comprehensive Cancer Center, Edwards Life Sciences Center for Advanced Cardiovascular Technology, Department of Biomedical Engineering, Department of Biological Chemistry, Department of Pharmaceutical Sciences, University of California Irvine, Irvine, CA, USA*
**egratton@uci.edu*

Abstract: Fluorescence-based single particle counting devices have become very powerful tools for human health-related applications such as the detection of blood-borne pathogens. Instead of passing the sample fluid through a thin tube or microfluidic chip, as it is commonly practiced in flow cytometers and sorter devices, single particle counters scan the fluid volume by rotation and translation of the sample container. Hence, single particle counters are not limited by the fluid flow friction and can scan a large volume in a short timeframe while maintaining high sensitivity. A single particle can be detected in a milliliter of the fluid sample within minutes, and diagnostics are being developed using this principle. Until now, signal detection with particle counters has been based on signal intensity and signal separation into multiple wavelength bands coupled with multiple detectors, which limits the number of species that can be resolved. In this paper, we applied fluorescence lifetime detection to single particle counting to increase specificity and enable multiplexing with a single detector. We demonstrate how this principle can be used for diagnostic assays based on fluorescence quenching.

1. Introduction

Single particle counting devices can be very powerful tools for human health centered applications due to their capability of detecting particles at extremely low concentrations from 1 to 10,000 particles per milliliter with exceptional robustness. As an example, it was previously demonstrated that bacteria can be detected with single-cell sensitivity in a single-step, culture- and amplification-free process within 1.5–4 h from milliliters of raw blood [1]. Rapid diagnostics such as this have great promise in better management of bloodstream infections and antibiotic treatment. In this type of particle counting device, the fluid sample is transferred into a cuvette that is rotated and translated in front of a lens focusing the illumination beam into the cuvette. The signal from a small observation volume is detected in a particular wavelength band with a fast detector such as a photomultiplier [2,3]. Because the sample volume is explored by moving the container rather than passing the fluid through a tube or channel the specimen is not subjected to turbulence or shear stress and a large volume can be processed in a short amount of time. Additionally, since the optical elements are not actuated, this technique is well suited for miniaturized, point-of-care instrumentation. While scattered light can be used to identify particles passing through the observation volume, the most popular approach is fluorescence labeling and detection due to its exceptional specificity and signal-to-noise ratio. A positive, fluorescently tagged particle passing through the detection volume will be registered as an intensity spike with the peak width proportional to

#354940 https://doi.org/10.1364/BOE.10.001223
Journal © 2019 Received 10 Dec 2018; revised 27 Jan 2019; accepted 27 Jan 2019; published 12 Feb 2019

Biomedical Optics EXPRESS

particle size convoluted with instrument parameters (observation volume geometry, cuvette rotational velocity and signal integration time). Based on this information the number of events can be counted and quantified as particle concentration. In addition, true "hits" can be separated from false positive "hits" generated by sample impurities if their sizes and/or shapes are sufficiently different. However, particle identification solely by peak width is limited, especially when unique targets are of comparable size. In addition, signal intensity, i.e., peak amplitude, is not a good criterion either since particles of the same brightness can produce very different amplitudes depending on their position within the detection volume which is not known unless the spatial information is encoded in the signal [4]. Hence, the most common approach to detecting different species is to label them with fluorophores of different excitation/emission properties and excite and detect them in multiple wavelength bands. The drawback of detecting different species in different color channels is an increase of the complexity of the particle counting device and the practical limitation to detection in <10 color channels [5]. More importantly, for fluorescence (de)quenching-based assays, commonly used in conventional fluorescence assays such as TaqMan PCR, the quenching molecule usually does not emit any fluorescence. Hence, without an acceptor fluorophore as quencher, target identification by color is not possible. Yet, the ability to detect fluorescence (de)quenching can be vital for the identification of DNA/RNA sequences as this is often the goal in single particle counting experiments. In such an experiment a DNA/RNA strand complementary to the target sequence is tagged with a fluorescent dye quenched by a second tag in close proximity to the fluorophore. Upon binding to the target sequence, the strand is unfolded or digested, leading to a spatial separation of fluorophore and quencher resulting in an increase in fluorescence quantum yield and lifetime. Combined with nucleic acid amplification methods such as PCR this enables the detection of pathogens in nucleic acid tests for the diagnosis of infectious diseases, hereditary/genetic diseases and cancers. Therefore, in this work, we describe the implementation and application of digital frequency domain (DFD) based fluorescence lifetime detection with a particle counting device. DFD lifetime detection uses the heterodyning principle in which the emission is translated to a cross-correlation frequency much lower than the frequency of the modulated illumination source allowing to minimize cost and complexity of the detection electronics. At the same time, high precision and 100% duty cycle ensures best possible use of the signal available. We further demonstrate how lifetime analysis of the data can be used to separate out sample impurities, distinguish populations of particles detected in a single color channel and how to orchestrate a fluorescence quenching-based assay with a single detector.

2. Lifetime detection with a particle counting device

Our particle counting setup for lifetime detection is based on a Quanta particle counting system (ISS, Champaign, IL, USA) and a FastFLIM data acquisition card (ISS). The individual components and data acquisition and analysis procedure are described in the following subsections.

2.1 Optics and mechanics

The system is based on a Quanta particle counter (ISS) with laser diode illumination (472 nm, ISS) and detection with photomultipliers (65816, Hamamatsu) as previously described [1]. Briefly, a motorized stage holds the cylindrical sample cuvette that can be rotated as well as translated at variable speeds. The excitation/detection unit is movable as well to optimize the position of the observation volume in the sample cuvette. The excitation beam is spectrally cleaned with a band pass filter (473/10 nm, Chroma), reflected off a dichroic mirror and focused into the sample cuvette by an objective lens (20x, NA 0.4, Newport). Fluorescence is collected with the same lens, split from the incident light by the dichroic mirror and filtered with a band pass filter (535/40 nm, Chroma) to exclude scattered excitation light. The fluorescence is then focused onto an aperture/pinhole (0.1-1 mm diameter) with a lens of 50

Biomedical Optics EXPRESS

mm focal length to suppress out-of-focus light before being detected by the photomultiplier. An overview of the optical path is shown in the top portion of Fig. 1.

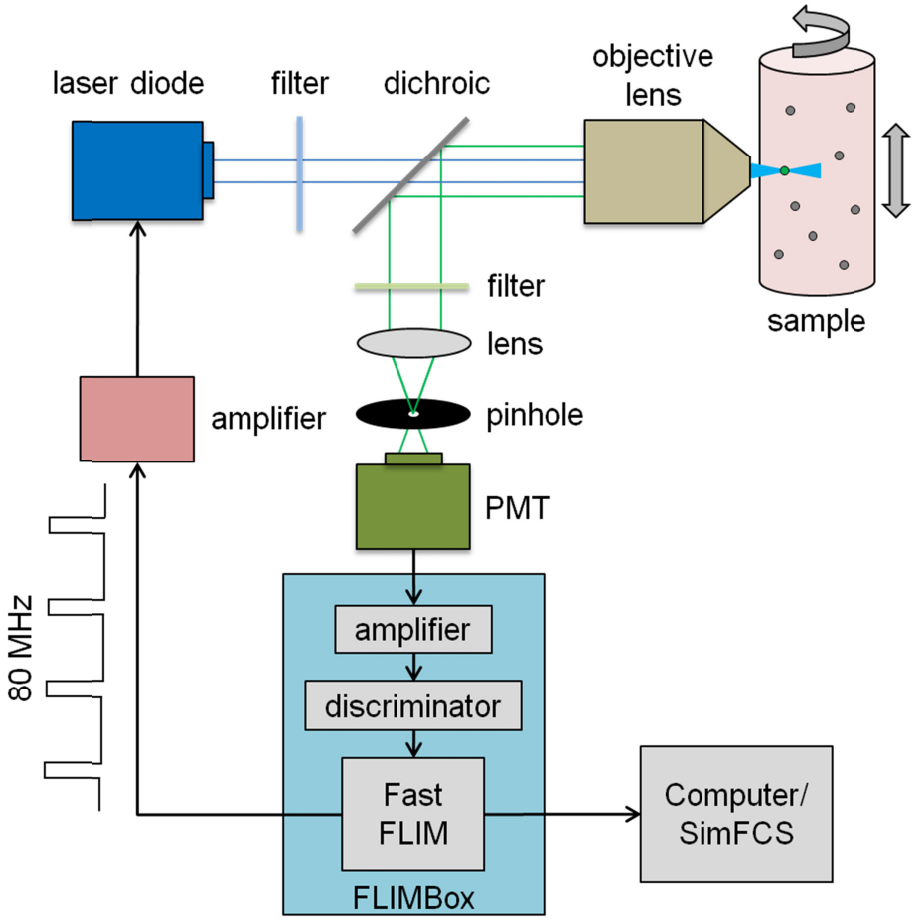

Fig. 1. Schematic of the particle counter setup as described in the text.

2.2 Electronics and data acquisition

A FastFLIM acquisition card (ISS) was used to generate a pulse train with pulses of 3 ns duration at a repetition rate of 20 or 80 MHz for laser modulation. The signal was amplified to an amplitude of 5 V with a high frequency amplifier (MHW6342T, Motorola) in order to maximize the modulation depth of the laser diode emission. The analog output signal of the PMT was first amplified by 30 dB with a high frequency amplifier (Model 50160, ISS) and then discriminated with a constant fraction discriminator (Model 6915, Phillips) to generate TTL pulses marking the arrival of a photon (photon counting). The use of photon counting allowed us to operate the PMT at very high gain (maximum sensitivity) while suppressing noise very efficiently. This step also converts the analog signal into a digital pulse train which can be processed by the FastFLIM acquisition card. An overview and schematic of the electronic setup are shown in the bottom part of Fig. 1. The FastFLIM acquisition card was operated and data was acquired with SimFCS software (Globals Software). Sample cuvette movement and PMT gain were controlled by ISS Quanta software.

Biomedical Optics EXPRESS

2.3 Digital frequency domain principle and data analysis

To measure the fluorescence lifetime we applied the principle of heterodyning in the digital frequency domain (DFD). As in the analog frequency domain approach a pulsed/modulated light source is used to illuminate the sample for a DFD lifetime measurement. However, instead of modulating the detector by, for example, time gating or gain modulation, the entire signal is collected. Instead, a time gate is applied digitally by splitting the detected signal into several windows, covering a certain time span of the excitation pulse period (here: four windows). This way a 100% duty cycle can be maintained. The frequency of those windows, f_s, is adjusted to be slightly different from the excitation pulse frequency, f_{ex}, resulting in a shift in window position with respect to the excitation signal as a function of time (Fig. 2(A)). This cross-correlation frequency, $f_{cc} = |f_s - f_{ex}|$, is much lower than the frequency of the excitation signal and thus requires less bandwidth. For each photon counted, a bin number, p, will be assigned depending on window number, w_n, and phase offset, p_{cc}, between sampling and excitation clocks,

$$p = (n_p - 1) - \left[\left(p_{cc} + \frac{n_p w_n}{n_w} \right) \bmod (n_p) \right], \tag{1}$$

with the number of phase bins, n_p, and the number of windows, n_w [6]. From the accumulated photon counts, a phase histogram of the lifetime response can be reconstructed (Fig. 2(B)). This phase histogram is a convolution of the lifetime decay, the square sampling window, the system jitter and the excitation pulse. To account for these parameters, a calibration data set with a fluorophore of known lifetime is measured. From this data, the position of the lifetime phase and modulation can be calculated and presented as a position on the phasor plot (Fig. 2(C)). The uncertainty of this position scales with the inverse of the square root of the number of photons collected. In a particle counting device the signal is recorded as a function of time. Particles crossing the observation volume create a peak in signal intensity (Fig. 2(D)). For peak identification, the data stream is analyzed with a cross-correlation filter as described previously [2]. In the data presented here we used a Gaussian model for the filter but it can be of any shape. For the photons accumulated during each peak extent the phase histogram is constructed (Fig. 2(E)) and the lifetime phase and amplitude is calculated for each particle (Fig. 2(F)). The lifetime data can then be used to discern between populations.

Biomedical Optics EXPRESS

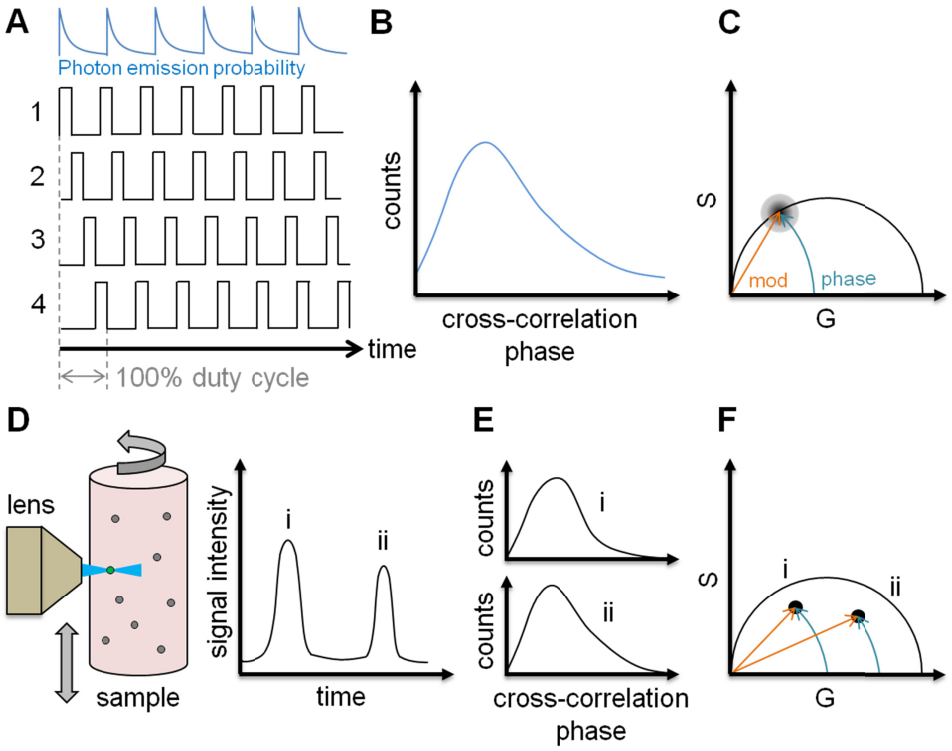

Fig. 2. Lifetime measurement with a particle counting device. (A) Principle of heterodyning, a pulsed/modulated light source is used to illuminate the sample, the photons detected are placed in certain bins with respect to the excitation pulse period. (B) From the counts accumulated in each bin, a phase histogram is constructed showing the average lifetime response. (C) From the phase histogram the lifetime phase and modulation can be calculated with the uncertainty scaling with the inverse of the square root of the number of photons collected. For each particle detected (D), the phase histogram is calculated (E) and transformed to a position on the phasor plot (F).

3. Results

To test the capabilities of our device we prepared and measured samples demonstrating how different populations of particles detected in a single color channel can be separated and how a fluorescence quenching-based assay can be measured with a single detector.

3.1 System calibration and testing with fluorescent droplets

To calibrate the system, we first measured a micromolar solution of the fluorescent dye Coumarin-6 dissolved in ethanol, which, under this condition, exhibits a fluorescence lifetime of 2.5 ns [7]. To test the system, a 1 µM solution of FITC was encapsulated in lipid droplets with an average diameter of 84 µm. Lipid droplets were formed as previously described in [1]. These droplets were diluted in a solution of unlabeled lipid droplets to a concentration of about 1 labeled droplet per 1,000 unlabeled droplets. This sample was subjected to lifetime data acquisition with the particle counter. Data was acquired for 30 s at a sampling rate of 50 kHz, cuvette rotation speed was 200 rpm and cuvette translation speed was 5 mm/s over a range of 2 mm, fluorescence was excited with 472 nm light modulated at 80 MHz and detected through a 535/40 nm band pass filter and focused into an aperture of 330 micrometer diameter before detection with the PMT. A one second long portion of the fluorescence intensity time trace is shown in Fig. 3(A), multiple high intensity events were visible. An exemplary peak indentified by application of the cross-correlation filter described in section 2

Biomedical Optics EXPRESS

is displayed on the millisecond timescale in Fig. 3(B). Figure 3(C) shows the cumulative phasor plot of all peaks identified in an overlay with the position of the lifetime established with the Coumarin 6 reference solution. Each blue dot represents the average phasor coordinates of the photons accumulated during each hit. The average lifetime of all peaks amounts to 4.0 ± 0.7 ns (from lifetime phase) and 3.7 ± 0.3 ns (from lifetime amplitude) which is in agreement with the expected value of 4.1 ns for FITC [8]. This also means that the lifetimes obtained from the phase and the amplitude are identical within the error of the measurement and, consequently, fall on the universal circle of the phasor plot (black semicircle in Fig. 3(C)). This is expected as FITC fluorescence lifetime follows a single exponential decay model.

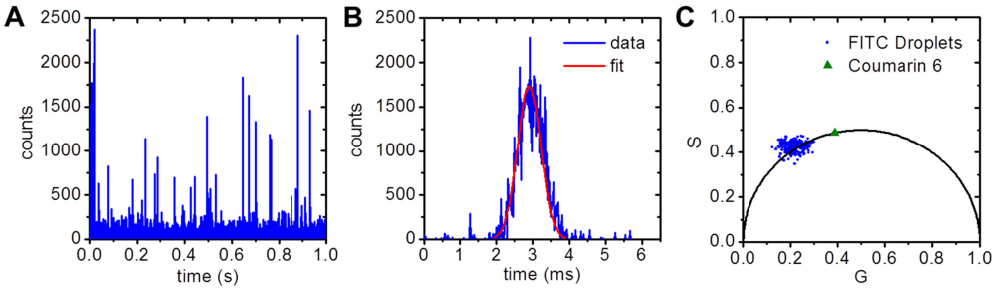

Fig. 3. (A) One second long portion of the fluorescence time trace of a solution of unlabeled lipid droplets mixed with FITC labeled droplets at a ratio of 1000 to 1. (B) Exemplary peak indentified with the correlation filter. (C) Cumulative phasor plot positions of all peaks identified overlaid with the position of the Coumarin 6 reference solution (2.5 ns). Each blue dot represents the average phasor coordinates of the photons detected for each hit.

3.2 Particle separation by lifetime

The goal of this experiment was to demonstrate how fluorescence lifetime measures can be used to distinguish two fluorophores with overlapping spectra that would not be distinguished by intensity alone. For this experiment, two droplet populations were generated, one containing the fluorescent dye FITC at a concentration of 1 µM, the other population containing the fluorescent dye Cy2 at a concentration of 10 µM (note that the quantum yield of Cy2 is ~7 fold lower than the quantum yield of FITC [9]).The fluorescence emission peak of FITC is shifted by only ~10 nm with respect to the emission peak of Cy2, hence, these two fluorophores would be extremely difficult to separate by color. The individual fluorescent droplet samples as well as a 1:1 mixture of both labeled droplets were diluted into solutions of droplets containing PBS only at a ratio of 1:1000. All three mixtures were subjected to lifetime data acquisition with the particle counter. A comparison of the resulting accumulated counts per particle and lifetimes after peak identification are shown in Fig. 4(A),(B). It can be seen that, while the average intensity for FITC droplets is higher than the average intensity of Cy2 droplets, it is not possible to fully separate individual droplets containing FITC from individual droplets containing Cy2 by means of fluorescence signal due to a wide distribution of intensities. The reason for these wide intensity distributions is that particles passing at the periphery of the observation volume will produce much less counts than an identical particle passing near the center of the confocal volume. Due to this overlap in intensity and emission spectrum, it is not possible to separate droplets containing FITC from droplets containing Cy2. However, leveraging the lifetime information, the two populations can be easily identified. The fluorescence lifetime is not affected by the spatial position of the particle with respect to the observation volume center. Only the precision at which the lifetime can be established depends on the number of photons, N, collected per event ($error \propto 1/\sqrt{N}$). Hence, particles passing at the periphery of the detection volume will have a larger error associated with their measured lifetimes. This kind of analysis could also be very useful for

Biomedical Optics EXPRESS

multiplexing. Instead or in addition to using markers with different excitation/emission spectra, several markers could be distinguished by lifetime in a single color channel. We note that as both, FITC and Cy2 exhibit single exponential lifetime decays, their phasor positions fall onto the universal circle. As the Cy2 droplets are relatively dim, the phasor distribution was pulled slightly towards the origin (0,0), the position of unmodulated background light.

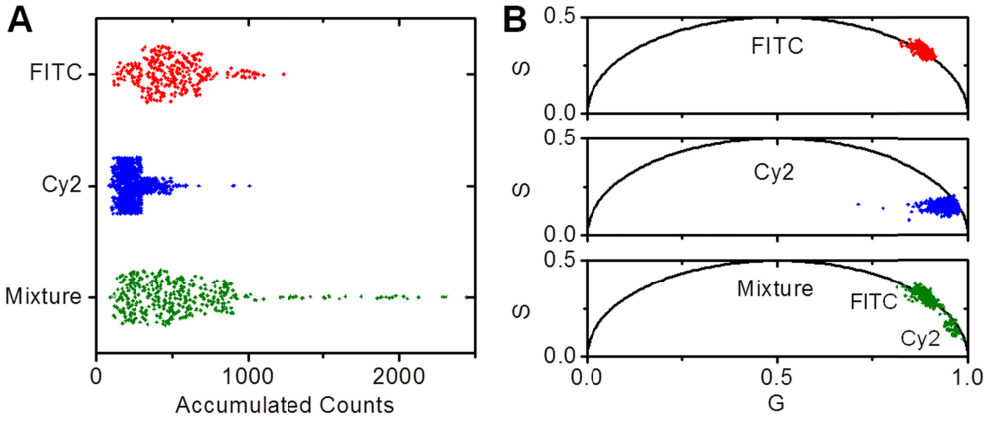

Fig. 4. (A) Comparison of peak intensities found for solutions of unlabeled lipid droplets mixed with lipid droplets containing FITC and Cy2, respectively. Each dot represents the total number of photons detected for a particle passing through the detection volume indentified by the correlation filter. (B) Comparison of peak lifetimes found for the data of the lipid droplet solutions presented in panel A. Clearly, the two populations can only be separated by lifetime, not intensity. Laser modulation frequency, 20 MHz.

3.3 Robust identification of sample contaminants

The particle counter is capable of detecting an extremely low number of particles (1-10) in a relatively large volume (1 ml). At this level, autofluorescent environmental contaminants such as dust particles present in the air can severely impact the measurement sensitivity by introducing false positive "hits". To overcome this problem, samples should ideally be prepared in a clean environment such as a cleanroom facility, but this limits field applications. As mentioned in the previous paragraph, peak amplitude is not a good criterion to distinguish multiple populations as particles passing at the periphery of the observation volume will produce much less fluorescence than an identical particle passing near the center of the confocal volume. Instead, false positive "hits" can be separated from true positive ones by means of signal intensity distribution (peak width) if the contaminant size significantly differs from the particles of interest. Unfortunately, this is not always the case. Yet, fluorescence lifetime is another parameter that can be exploited to distinguish different populations of particles. To investigate, we prepared a clean solution of 3 µm multispectral fluorescent microbeads (RFP-30-5, Sphereotech, Lake Forest, IL) and subjected it to particle counting with fluorescence lifetime detection. Then we contaminated the same solution with shelf dust and measured it again. The fluorescence intensities as well as lifetime distributions are shown in Fig. 5(A), (B). Clearly, it is not possible to identify "hits" due to sample contaminants by means of intensity, while, on the phasor plot, the two populations are immediately apparent. Hence, fluorescence lifetime detection is a robust tool to identify and exclude false positive "hits" due to sample contaminants. We note that the beads we used for this experiment contained multiple fluorophore species with different fluorescence lifetimes. Therefore, their position on the phasor plot does not fall onto the universal circle as it would for a single exponential decay but, instead, their positions reside inside the circle following the law of linear combination [10].

Biomedical Optics EXPRESS

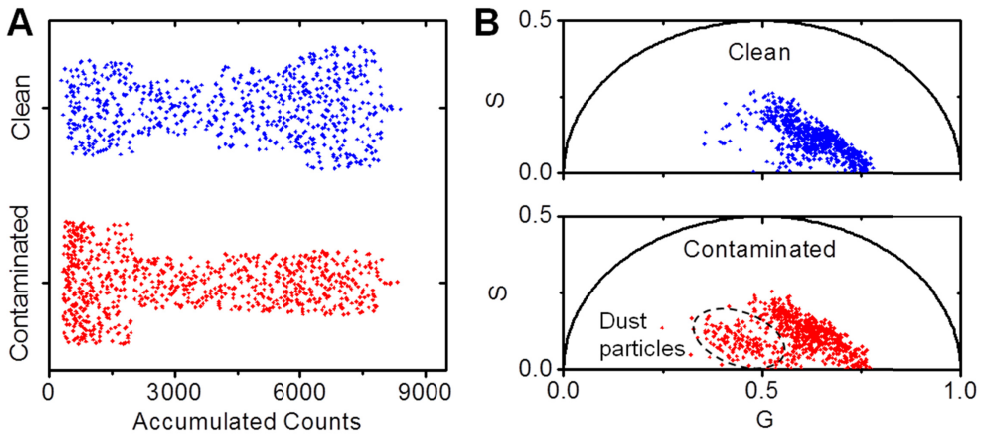

Fig. 5. (A) Comparison of peak intensities found for a solution of beads prepared in a clean environment with the same solution after adding shelf dust as contaminant. Each dot represents the photons counted while a particle was passing through the detection volume. (B) Comparison of peak lifetimes found for the data shown in panel A. Again, the two populations can only be separated by lifetime, not intensity. Laser modulation frequency, 20 MHz.

3.4 Detection of fluorescence (de)quenching by lifetime

In fluorescence quenching the emission of a fluorescence photon is suppressed because, in a particular environment, other means of energy conversion to relax the fluorophore into the ground state are preferred. This condition can be induced by a molecule, the quencher, in proximity to the fluorophore. Upon removal of the quencher, fluorescence emission is restored. This molecular switch can be engineered into a biosensor, for example, for application in a diagnostics assay. Probes such as TaqMan probes based on fluorescence quenching are the gold standard in the detection of DNA/RNA sequences. Fluorophore and quencher are attached to the complementary DNA/RNA sequence of interest and in close proximity to each other in the folded, unbound state. Upon binding to the target sequence, the strand is unfolded spatially or digested removing the quencher from the fluorophore resulting in a drastic change of the fluorescence quantum yield. Hence quenching changes both the fluorescence intensity and the fluorescence lifetime. An example of such a system is shown in Fig. 6. Lipid droplets from a TaqMan assay to detect the presence of KRAS G12D mutant targets were prepared with either no target present (negative sample), or with the synthetic mutant target at a concentration of 700,000 copies/ml (positive sample). By partitioning each sample into millions of picoliter-sized droplets, the negative sample was composed of only quenched dye droplets while the positive sample was composed of a mix of quenched dye droplets and unquenched dye droplets. With the sample containing only droplets with quenched dye (negative sample), the intensity and lifetime can be established for this population. The goal regarding the sample containing droplets with quenched and unquenched dye is to reliably separate the two populations minimizing false positive as well as false negative events. The intensity distributions of the negative and positive samples are plotted in Fig. 6(A). While the distribution is shifted towards higher intensities as expected for the positive sample, no clear boundary between low intensity droplets with a high fraction of quenched probes and high intensity droplets with a high fraction of unquenched probes can be found. Again the reason is that the same particle passing the excitation volume at the center will produce a different intensity compared to passing the periphery. Figure 6B shows the lifetime distributions of the same samples on the phasor plot. For fully quenched probes the fluorescence lifetime approaches zero represented by the 1,0 (G,S) position on the phasor plot. However, this value can never be measured since a fully quenched probe would not emit any fluorescence. Still, this boundary condition can be used to extrapolate the quenching

Biomedical Optics EXPRESS

trajectory as indicated by the dotted line where the fully unquenched position is determined by the lifetime of the free dye. From the position of each event along the quenching trajectory, the fraction of unquenched probes can be determined as shown in Fig. 6(C). It can be seen that the distribution of lifetimes is very different from the distributions of intensity. Although still overlapping, the presence of two populations (quenched/unquenched) is suggested by the dip in frequency of "hits" at the center of the distribution (indicated by arrows). To compare the results obtained by fluorescence lifetime with the results obtained by intensity, the two parameters are plotted against each other in Fig. 6(D). From the events detected in the negative sample (all quenched), the median values and standard deviations (SDs) of the fraction unquenched determined by lifetime (0.502 ± 0.063) as well accumulated counts per event (669 ± 159) were calculated. The median values plus SDs (fraction unquenched: 0.565, accumulated counts: 828) could serve as thresholds to distinguish positive from negative events in the positive sample and are plotted as dotted lines dividing Fig. 6(D) into four quadrants. As both lifetime and intensity increase during a transition from the quenched to the unquenched state, the distribution of events should follow a linear trajectory from quadrant 1 to quadrant 3. This is not the case. Instead, the distribution shows a curvature where events with a lower intensity but longer lifetime (quadrant 2) are much more frequent than events of high intensity but shorter lifetime (quadrant 4). This shows that the intensity value is compromised by the particle position within the observation volume while the lifetime is not. Hence, for this sample, the fluorescence intensity alone is not a reliable criterion to analyze fluorescence quenching. By adding lifetime analysis, on the other hand, it is possible to identify the different states with higher specificity. To quantify this difference in specificity we calculated the number of events residing in quadrants 2 and 4. Assuming that either a higher intensity or a longer lifetime indicate the presence of an unquenched dye droplet (positive "hit"), we counted 66 positive events detected by intensity but missed by lifetime versus 179 positive events detected by lifetime but missed by intensity resulting in a ratio of 2.7 for the detection of otherwise false negative events by intensity versus lifetime. This would be very useful for the design of an assay in which false negative events are important to exclude. On the other hand, for a test demanding low false positives, the events located in quadrant 3 are of interest as a positive event is confirmed by both, high fluorescence intensity and long lifetime lowering the probability of a false positive. We noticed that the phasor plot position of the negative, quenched droplet sample was relatively far from the position expected for a fully quenched probe. While this is in agreement with the frequent occurrence of "hits" representing quenched droplets during particle counting, we acquired fluorescence lifetime microscopy (FLIM) images for further investigation. A small volume of positive sample was loaded onto a counting slide and subjected to FLIM. The intensity image is presented in Fig. 6(E). The corresponding FLIM image with the pixels color coded according to their phasor plot positions is shown in Fig. 6(F). The two cursors in Fig. 6(G) mark the positions of the negative (cyan) and positive (magenta) droplets. Pixels within the perimeter of those cursors were painted accordingly in the FLIM image. It can be seen that the phasor plot position of the negative droplets measured by FLIM is in excellent agreement with the data obtained by particle counting and the relatively high signal from negative droplets is a consequence of the probe design. This underlines the strength of lifetime detection with particle counting devices.

Biomedical Optics EXPRESS

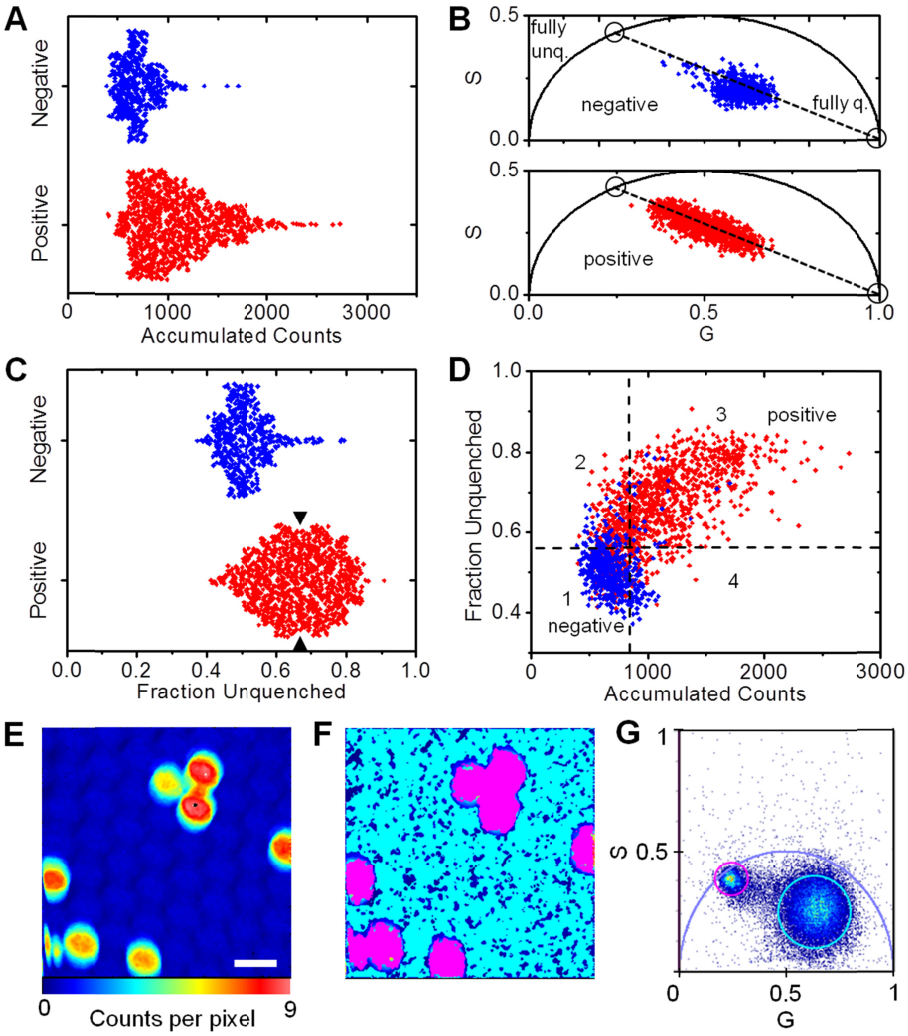

Fig. 6. Lifetime analysis of Kras3.0 quenched droplets (negative) and Kras3.0 quenched droplets mixed with unquenched droplets (positive) data acquired with the particle counter. (A) Intensity distribution of the "hits" detected for the negative and positive sample, each dot represents the photons counted for a given particle passing through the detection volume. (B) Phasor plot distributions of lifetimes of the "hits" detected for the negative and positive samples. The dotted line indicates the quenching trajectory from fully unquenched to fully quenched with the limits indicated by circles on the phasor plot. (C) Distribution of the positions of the "hits" detected along the quenching trajectory. Arrows indicate the boundary between quenched and unquenched populations. (D) Plot of "hit" quenching trajectory positions as a function of "hit" intensity. The median values plus standard deviations of the intensity and fraction unquenched determined by lifetime of the negative sample are represented by dotted lines, dividing the plot area in quadrants 1-4. (E) Fluorescence microscopy image of the positive sample. (F) Corresponding FLIM image with the pixels color coded according to their phasor plot positions shown in panel G. (G) Phasor histogram of pixel lifetimes. Two cursors mark the positions of the quenched (cyan) and unquenched (magenta) dye. Pixels within the perimeter of those cursors are painted accordingly in panel F. Laser modulation frequency, 80 MHz. Scale bar, 100 µm.

4. Discussion

Our prototype particle counter is equipped with two detection channels. In the future, we intend to use two excitation wavelengths to excite dyes of different absorption/emission

Biomedical Optics EXPRESS

properties. By pulsing the lasers in an alternating fashion, crosstalk between detection channels can be avoided [11]. Hence, the presence of two dyes on the same target can be identified. Further, we propose that instead or in addition to lifetime measurements, spectrally resolved detection could be used with particle counting devices including spectral phasor-based analysis. While fluorescent markers of similar emission spectrum are difficult to distinguish by fluorescence intensity or color, they can be clearly separated by lifetime if significantly different. With phasor-based analysis even small differences can be resolved with only little fluorescence signal. Hence, we propose unmixing of a large number of species (3-10) by lifetime. Fluorescence resonance energy transfer (FRET) is a special form of fluorescence quenching in which the energy of one dye, the donor, is transferred to another dye, the acceptor, over short distances (0.1-1 nm). Since FRET affects the fluorescence lifetime, we propose to use FRET dye pairs as sensors for biomedical applications with particle counting devices.

Funding

National Institutes of Health (NIH) (R01AI117061, P41 GM103540, P50 GM076516); UC Irvine Applied Innovation's POP grant.

Acknowledgments

We would like to thank Chenyin Ou and Jonathan Grunwald from Velox Biosystems Irvine for kindly providing the KRAS G12D lipid droplet samples.

T.V. is supported by NSF Graduate Research Fellowships Program (GRFP).

Disclosures

Enrico Gratton, Per Niklas Hedde and Weian Zhao: University of California Irvine, US Patent Application No.: (P). W.Z. is a founder of Velox Biosystems Inc that develops in vitro diagnostics.

References

1. D. K. Kang, M. M. Ali, K. Zhang, S. S. Huang, E. Peterson, M. A. Digman, E. Gratton, and W. Zhao, "Rapid detection of single bacteria in unprocessed blood using Integrated Comprehensive Droplet Digital Detection," Nat. Commun. **5**(1), 5427 (2014).
2. J. P. Skinner, K. M. Swift, Q. Ruan, S. Perfetto, E. Gratton, and S. Y. Tetin, "Simplified confocal microscope for counting particles at low concentrations," Rev. Sci. Instrum. **84**(7), 074301 (2013).
3. I. Altamore, L. Lanzano, and E. Gratton, "Dual channel detection of ultra low concentration of bacteria in real time by scanning FCS," Meas. Sci. Technol. **24**(6), 65702 (2013).
4. M. Bouzin and E. Gratton, "Multi-slit detection," (patent pending).
5. S. P. Perfetto, P. K. Chattopadhyay, and M. Roederer, "Seventeen-colour flow cytometry: unravelling the immune system," Nat. Rev. Immunol. **4**(8), 648–655 (2004).
6. R. A. Colyer, C. Lee, and E. Gratton, "A novel fluorescence lifetime imaging system that optimizes photon efficiency," Microsc. Res. Tech. **71**(3), 201–213 (2008).
7. E. Terpetschnig and D. M. Jameson, "Fluorescence Lifetime," (ISS Inc., 2005).
8. ISS, "Lifetime Data of Selected Fluorophores," (ISS Inc., 2018).
9. G. T. Dempsey, J. C. Vaughan, K. H. Chen, M. Bates, and X. Zhuang, "Evaluation of fluorophores for optimal performance in localization-based super-resolution imaging," Nat. Methods **8**(12), 1027–1036 (2011).
10. S. Ranjit, L. Malacrida, D. M. Jameson, and E. Gratton, "Fit-free analysis of fluorescence lifetime imaging data using the phasor approach," Nat. Protoc. **13**(9), 1979–2004 (2018).
11. B. K. Müller, E. Zaychikov, C. Bräuchle, and D. C. Lamb, "Pulsed interleaved excitation," Biophys. J. **89**(5), 3508–3522 (2005).